Chapter 13

Bioluminescence Microscopy: Design and Applications

Hirobumi Suzuki, May-Maw-Thet, Yoko Hatta-Ohashi, Ryutaro Akiyoshi and Taro Hayashi

Additional information is available at the end of the chapter

http://dx.doi.org/10.5772/65048

Abstract

Bioluminescence imaging by microscopy is performed using an ultra-low-light imaging camera. Although imaging devices such as sensor and camera have been greatly improved over time, such improvements have not been attained commercially which are available for microscopes now. We previously optimized the optical system of a microscope for bioluminescence imaging using a short-focal-length imaging lens and evaluated this system with a conventional color charge-coupled device camera. Here, we describe the concept of bioluminescence microscope design using a short-focal-length imaging lens and some representative applications, including intracellular calcium imaging, imaging of clock gene promoter assays, and three-dimensional reconstruction of *Drosophila* larva. This system facilitates the acquisition of bioluminescence images of single live cells using luciferase, which is similar to fluorescence microscopy using a fluorescent protein.

Keywords: bioluminescence microscopy, short-focal-length imaging lens, single live-cell analysis, three-dimensional imaging

1. Introduction

Aequorin is a calcium-specific light-emitting protein extracted from the jelly fish *Aequorea* [1]. Additionally, aequorin-injected eggs of the medaka (*Oryzias latipes*), a fresh water fish, showed a dramatic increase in free calcium during fertilization, as determined by measuring light from the eggs using a photomultiplier tube [2]. Notably, bioluminescence microscopy with an image intensifying system using a vidicon camera was performed in 1978 to show the spatial distri-

bution of the free calcium in the egg [3]. This system revealed a spreading wave of high free calcium (calcium wave) during fertilization from the animal pole, as discussed with the fertilization wave of cortical changes in eggs observed by light microscopy [4]. Although the potential of low-light imaging has been recognized in physiology and developmental biology, this technique was not commonly used at that time due to a lack of commercially available instrumentation. Later, advances in detector and digital imaging processing systems facilitated the commercial production of appropriate instrumentation and made it possible for low-light imaging to be carried out using a silicon-intensifier target (SIT) tube camera or a high-sensitivity cooled charge-coupled device (CCD) camera.

Since the cloning of firefly luciferase in the late 1980s, luciferase has been used as a reporter enzyme to assay the activity of a particular gene promoter using the photon-counting luminometer method [5–7]. Additionally, bioluminescence microscopy of promoter activity in single cells has been performed using ultra-low-light imaging cameras, such as liquid nitrogen-cooled CCD cameras, photon-counting CCD cameras, or image-intensifying CCD cameras [8–16]. However, temporal and spatial resolution was not enough for the observation of cellular biological events and for the detection of single cells compared with that of conventional CCD cameras. Therefore, satisfactory analysis has not been achieved at the single-cell level by bioluminescence microscopy.

Recently, electron-multiplying CCD (EM-CCD) camera, which yields higher sensitivity and image quality, was commercially released and subsequently used for bioluminescence microscopy [17–19]. Although the image sensor of ultra-low-light imaging cameras has been greatly improved over time, such improvements have not been made commercially available for microscopes.

In our previous studies, we optimized an optical system using a short-focal-length imaging lens for bioluminescence microscopy and performed bioluminescence imaging of single live cells expressing the luciferase gene using a conventional CCD camera [20, 21]. This system is commercially available now and has been widely used for gene expression analysis in chronobiology [22–28], neurobiology [29, 30], developmental biology [31], medical research [32–35], signal transduction analysis [36–38], molecular interaction [39–41], and radiation biology [42, 43]. Accordingly, in this study, we describe the concept of bioluminescence microscopy adopting a short-focal-length imaging lens and present several representative applications, including a three-dimensional analysis, to demonstrate the advantages of the short-focal-length imaging lens system.

2. Microscope design

Bioluminescence microscopy is based on the detection of light emitted by living cells expressing a luciferase gene or other luminescence-related gene. Conventional microscopes are inefficient at transmitting light from the sample to the detector, necessitating long exposure times. We designed a new type of microscope for ultra-low-light imaging based on modifications to the imaging lens, vignetting, and effective field area.

http://dx.doi.org/10.5772/65048

2.1. Imaging lens

Figure 1 shows a diagram of an inverted microscope equipped with an infinity-corrected optical system. Light from a sample is collected by an objective lens (OB), and the sample image is created by an imaging lens (tube lens; IM) on a CCD chip. Generally, the degree of brightness (I) of an image is directly proportional to the square of the numerical aperture (NA) of the OB and is inversely proportional to the square of magnification (M) of the image, namely as $I \propto (NA/M)^2$. Therefore, a higher NA and lower M yield much brighter images. However, it is difficult to obtain both conditions. Because higher NA OB yields higher M (shorter focal length), or lower M OB yields lower NA. Thus, high NA and low M are mutual trade-offs. On the other hand, the value of NA/M is the same as the NA of the IM, geometrically denoted as NA′. Therefore, a microscope with a high NA′ (short-focal-length imaging lens) makes it possible to achieve a higher NA and lower M without further improvement of the objective lens. This was the concept on which we based the design of the bioluminescence microscope [20, 21].

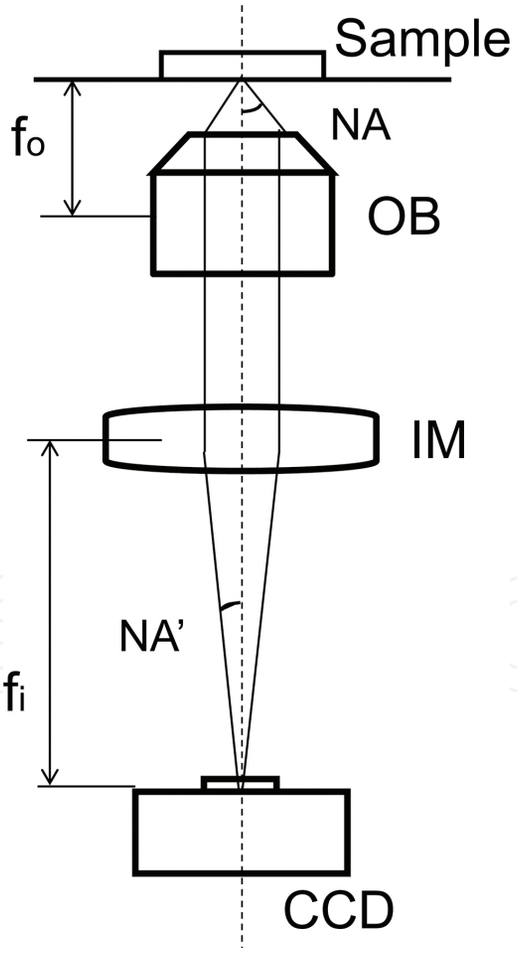

Figure 1. A diagram of an inverted microscope with an infinity-corrected optical system. OB, objective lens; IM, imaging lens; NA, numerical aperture of the objective lens; NA′, numerical aperture of the imaging lens; F_o, focal distance of the objective lens; F_i, focal distance of the imaging lens.

Figure 2 shows one example of the I condition to capture bioluminescence images of live cells using a microscope. The X-axis indicates the I value of the *in vivo* macro-imaging system, OV100 (Olympus, Tokyo, Japan), using a 0.8× objective lens with an NA varying from 0.05 to 0.25 (I = 0.004–0.098). HeLa cells transiently expressing the Luc+ luciferase gene (pGL3 control vector; Promega, Madison, WI, USA) in Hanks' balanced salt solution (HBSS; Invitrogen, Carlsbad, CA, USA) containing 1 mM D-luciferin, potassium salt (Promega) at room temperature were imaged using a CCD camera (ST-7; SBIG, Ottawa, Canada) for astronomical imaging. The exposure time was 1 min, and the cooling temperature was −20°C. The Y-axis indicates the normalized luminescence intensity of the entire area of the image captured (**Figure 2A**). As shown in the graph (**Figure 2B**), luminescence images could be captured at I values of greater than 0.02, although the M was lower for single-cell imaging. Therefore, we designed an IM to achieve an I value of 0.02 with a higher M using a conventional OB.

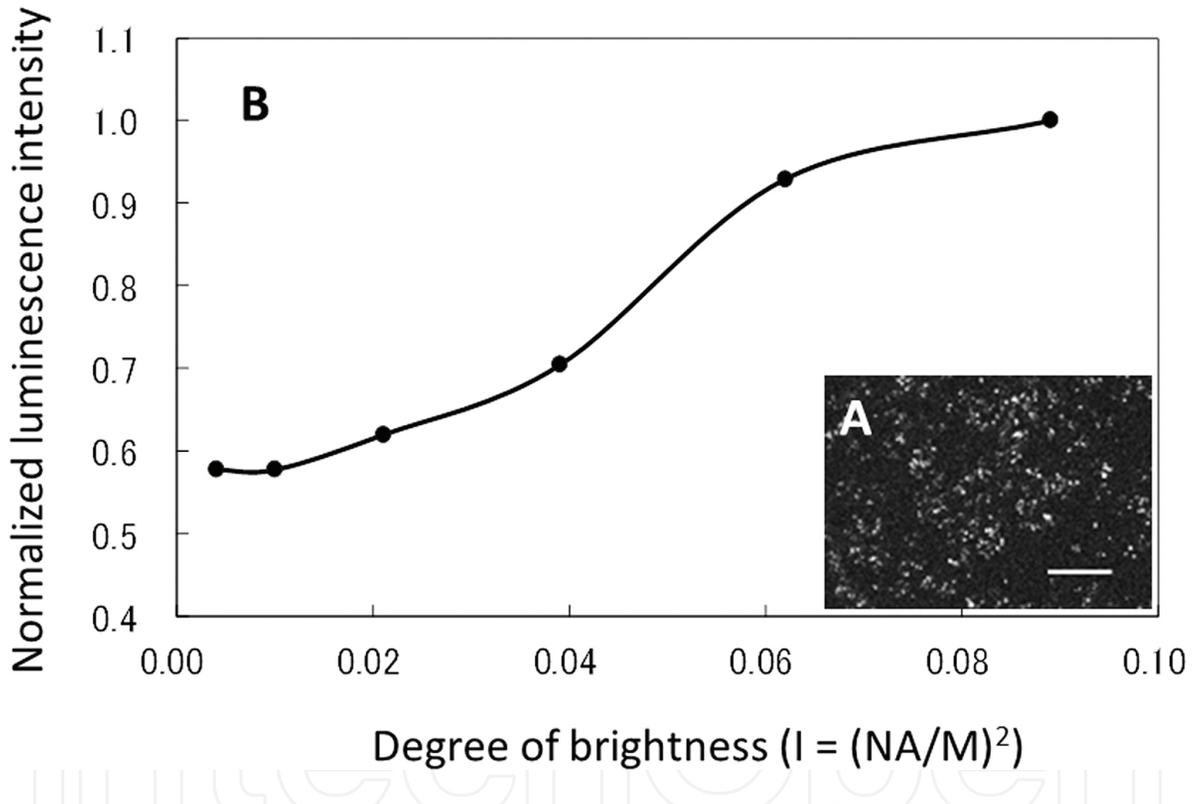

Figure 2. The I condition to capture bioluminescence images of HeLa cells using an OV100 *in vivo* macro-imaging system with a 0.8× objective lens and an NA ranging from 0.05 to 0.25 (I = 0.004 to 0.098). (A) HeLa cells expressing the Luc+ luciferase gene in HBSS containing 1 mM D-luciferin. Scale bars, 1000 μm and (B) normalized luminescence intensity of the image (A) against degree of brightness I.

2.2. Vignetting

Figure 3 shows diagrams of light passing from an object in an infinity-corrected optical system. In this system, light from object runs parallel between the OB and IM (**Figure 3A** and **B**). Therefore, this system is suitable for several observations because several optical elements (such as mirror units for fluorescence observations or polarizing filters) can be inserted

http://dx.doi.org/10.5772/65048

between the OB and IM without light-pass correction for image formation. However, light from peripheral vision (ray "a") is vignetted by the imaging lens, when the distance between the OB and IM becomes longer (**Figure 3C**). Therefore, vignetting can be avoided by shortening the distance between the OB and IM.

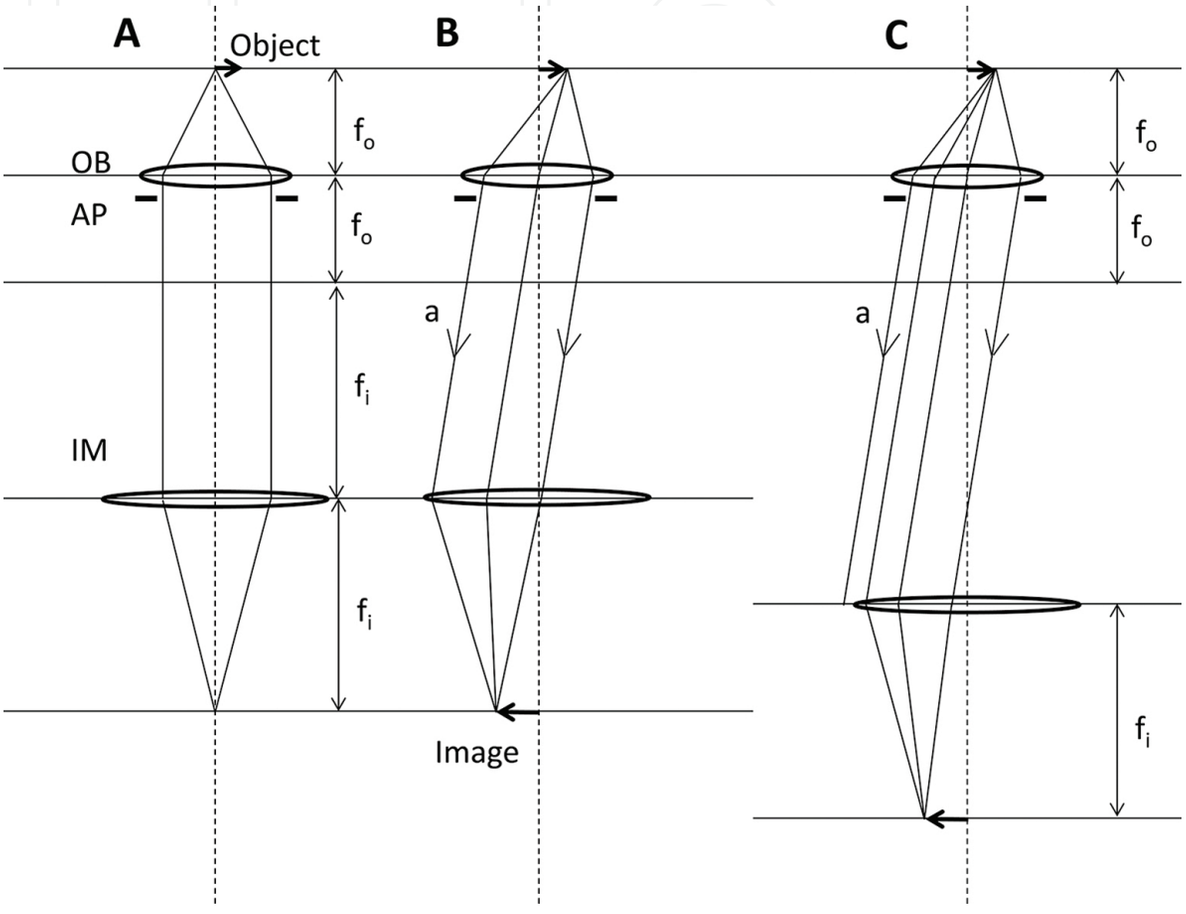

Figure 3. Diagrams of light passing from an object in an infinity-corrected optical system, illustrating the vignetting of light from peripheral vision by the imaging lens. (A) Light passing through the central axis. Light flux was restricted by the aperture of the objective lens; (B) light passing through peripheral vision; and (C) light passing through peripheral vision when the distance between the objective and the imaging lens was greater than that in B. Light from peripheral vision (ray "a") was vignetted by the imaging lens. OB, objective lens; AP, aperture; IM, imaging lens; f_o, focal distance of the objective lens; f_i, focal distance of the imaging lens.

2.3. Effective field area

Figure 4 shows an effective field diagram on a CCD chip. Generally, the area of the CCD chip is smaller than the effective field area because peripheral vision is affected by several optical aberrations. Images on the CCD chip only show part of the light collected by the OB. If all light is collected on the CCD chip as an image by reducing the magnification using an intermediate tube lens or modified IM, the light intensity of each pixel becomes greater. Thus, image quality is sacrificed to obtain brighter images.

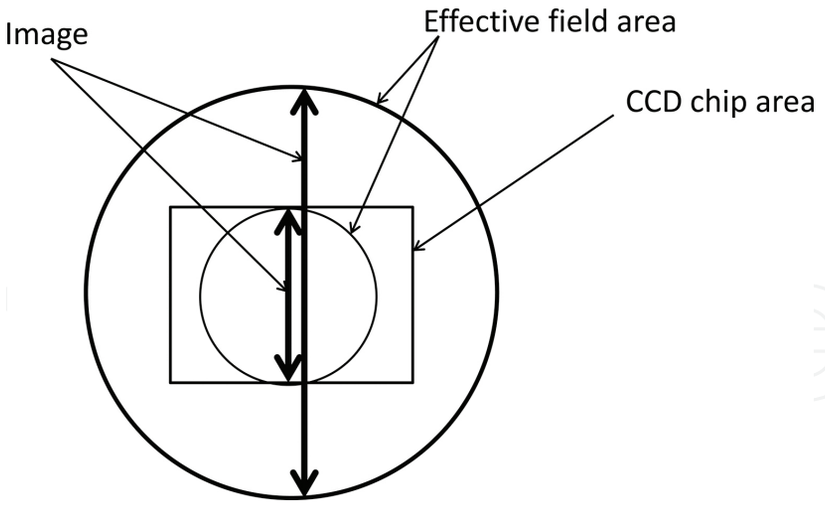

Figure 4. An effective field diagram on a CCD chip. Generally, the area of a CCD chip is smaller than the effective field area, and an image on a CCD chip is only some of light collected by the objective lens. If all light is collected on the CCD chip as an image by reducing the magnification using an intermediate tube lens or modified imaging lens, the light intensity of a pixel of the CCD chip increases.

2.4. The bioluminescence microscope, LV200

Figure 5 shows the inverted bioluminescence microscope used in our studies (Luminoview LV200; Olympus, Tokyo, Japan). A halogen lamp was used as the source of transmitted bright-field light. The light was directed to a sample through a condenser lens with a glass fiber. A short focal-length imaging lens (f = 36 mm, NA = 0.2) was customized based on the condition of I to capture dim bioluminescence images in this system. Normal OBs are available for observation. Using the IM, total magnification was reduced to one-fifth of the magnification of the OB because the focal distance of the IM is fixed (180 mm; Olympus) in a conventional microscope body. The distance between the OB and IM was set at 17 mm to avoid vignetting. A stage-top incubator with temperature and CO_2 gas controllers (MI-IBC-IF; Tokai Hit Co., Shizuoka, Japan) was added to the sample stage. The observation area was covered with a dark box [21, 44].

To evaluate the performance of LV200, bioluminescence images of U2OS cell lines stably expressing CBG99, CBR, and Luc2 beetle luciferase (Promega) were captured using an UPlanFLN 40× oil objective lens (NA = 1.30, I = 0.026) and DP70 color CCD camera (Olympus). Cells were cultured on 35-mm glass-bottomed dishes in Dulbecco's modified Eagle's medium (DMEM; Invitrogen) containing 10% fetal bovine serum and 1 mM beetle D-luciferin at 37°C with 5% CO_2. Binning of the CCD camera was 1 × 1 (1360 × 1024 pixels), International Organization for Standardization gain was 1600, and exposure time was 2 min. **Figure 6A** shows the bioluminescence images of cells expressing CBG99, CBR, and Luc2, captured within 2 min using a conventional color CCD camera as green, red, and orange color, respectively. Notably, bioluminescence images could not be captured under the same conditions (stable cell lines, OB, CCD camera, and exposure time) using a conventional inverted microscope (IX70; Olympus; NA = 1.30, I = 0.001), although a 10-min exposure time was required to obtain images

http://dx.doi.org/10.5772/65048

for the beetle luciferase-expressing cell line (**Figure 6B**) [21]. Despite the use of blank image subtraction, 10 min is the upper limit of exposure time for the DP70 color CCD camera due to intense background evaluation [21]. Thus, bioluminescence images of cells expressing the luciferase gene can be captured using an LV200 microscope with a 40× OB and color CCD camera. In this case, the M of the image was reduced by a power of 8 owing to the short-focal-length IM, and the I value was 0.026. To equalize the I value between the LV200 and IX70 microscopes, a low M and high NA OB (e.g., 8×, NA 1.3) is required for IX70. However, an OB with such a high NA cannot be purchased commercially.

Figure 5. Bioluminescence microscope, LV200. A stage-top incubator with temperature and CO_2 gas controllers was added to the sample stage. The observation area was covered with a dark box.

To show the spatial resolution of the bioluminescence images acquired using LV200, organelle-targeted images were captured using an UPlanFLN 100× oil objective lens (Olympus) and ImagEM EM-CCD camera (C9100-13; Hamamatsu Photonics, Shizuoka, Japan). The binning of the EM-CCD camera was 1 × 1 (512 × 512 pixels), EM-gain was 1024, and exposure time was 300 ms to 1 s. NanoLuc luciferase (Promega), which is 150-fold brighter than beetle luciferase [37], was used as a tag for organelle localization, similar to a fluorescent protein. Before substrate addition (12.5 μM furimazine; Promega), cells were washed with culture medium three times.

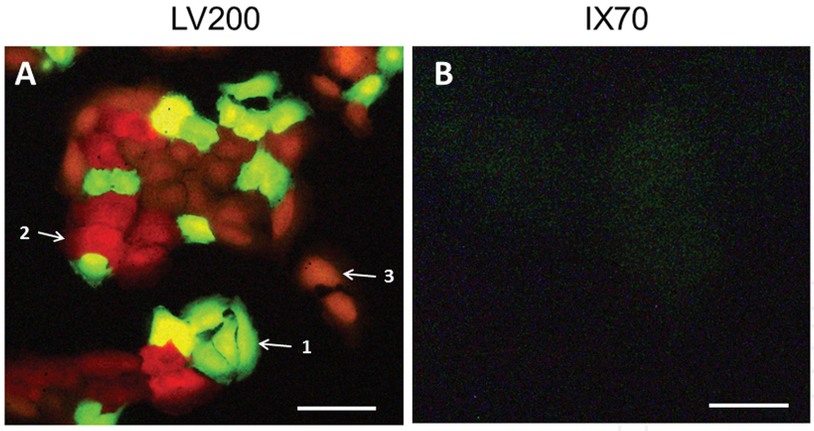

Figure 6. Bioluminescence images of U2OS cells expressing beetle luciferase CBG99 (arrow 1), CBR (arrow 2), and Luc2 (arrow 3) at 37°C captured by LV200 and IX70 microscopes with a UPlanFLN 40× oil objective lens and DP70 color CCD camera. The exposure times were 2 and 10 min for LV200 (M = 8, I = 0.026) and IX70 (M = 40, I = 0.001), respectively. D-Luciferin, 1 mM. Scale bars, 100 μm (A) and 20 μm (B). This figure was quoted and modified from Ref. [21] with Wiley's open access terms and conditions.

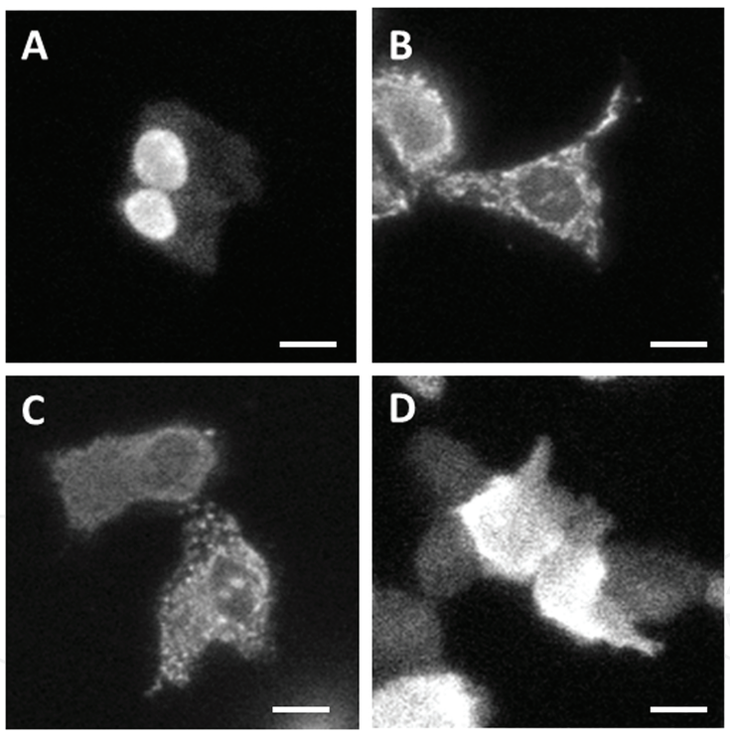

Figure 7. Bioluminescence images of NanoLuc fused with NLS (A), CoxVIII (B), calreticulin (C), and no targeting sequence (D) in U2OS cells at 37°C. Images were captured using an LV200 microscope with an UPlanFLN 100× oil objective lens and an ImagEM EM-CCD camera. Exposure time, 300 ms (A, D), 500 ms (B), and 1 s (C). Furimazine, 12.5 μM. Scale bars, 20 μm. This figure was quoted from Ref. [21] with Wiley's open access terms and conditions.

Figure 7 shows bioluminescence images of NanoLuc fused with nuclear localization sequence (NLS) (**Figure 7A**), mitochondrial targeting sequence (subunit VIII of human cytochrome C oxidase, CoxVIII) (**Figure 7B**), endoplasmic reticulum resident protein, calreticulin

with KDEL retrieval sequence (**Figure 7C**), or no targeting sequence (**Figure 7D**) in U2OS cells [21]. The NanoLuc-NLS accumulated in the nucleus of the cell, and the CoxVIII-NanoLuc and calreticulin-NanoLuc-KDEL appeared in a meshwork pattern in the cytoplasm. Thus, the nucleus and cytoplasm were discriminated clearly, and mitochondria and endoplasmic reticulum were recognized in the cytoplasm.

3. Applications

As examples of bioluminescence microscopy using our system (LV200), we introduce three applications: (1) calcium imaging of single cells, (2) imaging of clock gene promoter assays, and (3) three-dimensional imaging of *Drosophila* larva.

3.1. Intracellular Ca^{2+} imaging using obelin

Obelin is a calcium-specific bioluminescent protein similar to aequorin; using obelin, intracellular calcium was imaged by ATP and ionomycine (A23187) stimulation for calcium release from intracellular membranes (mitochondria and endoplasmic reticulum) and inflow from outside of the cell, respectively. The apoobelin gene [45] was inserted into the mammalian expression vector, pCDNA3.1 (Invitrogen), and transfected into HeLa cells. HeLa cells transiently expressing apoobelin were incubated in DMEM containing 60 μM coelenterazine (Promega) for 4 h to reconstitute obelin. The cells were stimulated with 500 μM ATP, and bioluminescence images were captured using an LV200 microscope with an UplanApo 20× OB (NA = 0.70; Olympus) and an iXon EM-CCD camera (DU-897l; Andor Technology, Belfast, UK). Binning of the CCD was 2 × 2, EM gain was maximum, and the exposure time was 25 s with a 30-s interval. The cells were restimulated by 10 mM ionomycine at 20 min after ATP stimulation.

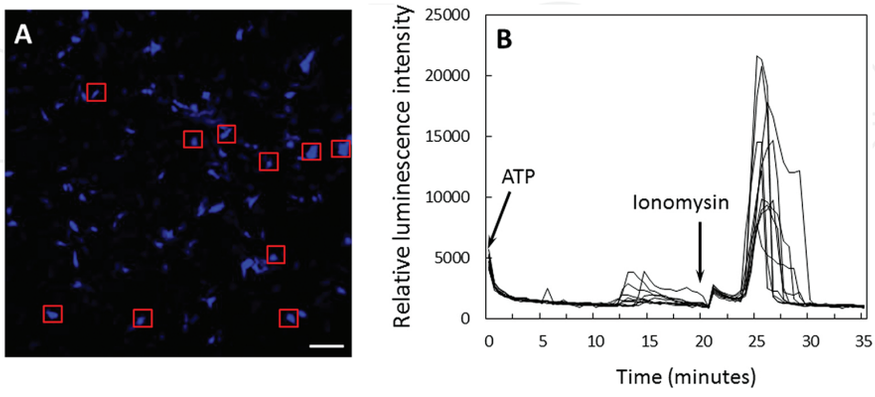

Figure 8. Bioluminescence image of intracellular calcium levels in HeLa cells using the photoprotein obelin (A). Time course of light intensity in single cells (B). Images were captured using an LV200 microscope with an UPlanApo 20× objective lens and an ImagEM EM-CCD camera. Cells were stimulated with 500 μM ATP and 1 mM ionomycine. Coelenterazine, 60 μM. Exposure time, 25 s. Scale bar, 200 μm.

Figure 8A shows pseudocolor-coded bioluminescence images of intracellular calcium in HeLa cells at 8 min after ionomysin stimulation. **Figure 8B** shows a time course of the intracellular calcium response for 10 single cells using time-laps image analysis software TiLIA [46]. Calcium responses in each cell varied temporally, were broad in intensity at around 15 min after ATP stimulation, and were uniform and greater in intensity after ionomysin stimulation [47, 48]. Using this imaging system, ATP-induced calcium oscillation in HEK-293 cells was confirmed using a bioluminescent calcium sensor constructed by aequorin and GFP with 1 s exposure time using a bioluminescence resonance energy transfer (BRET) system [36].

3.2. Imaging of clock gene promoter assays

The circadian rhythm is monitored by measuring the promoter activity of clock genes from individual cells as a cellular clock. However, it is impossible to resolve whether loss of circadian rhythm following stimulation is caused by dis-periodicity or dis-synchronicity in individual cells using a luminometer because the luminometer captures total luminescence from the cell population. Bioluminescence microscopy can provide clear single-cell analyses of promoter activity.

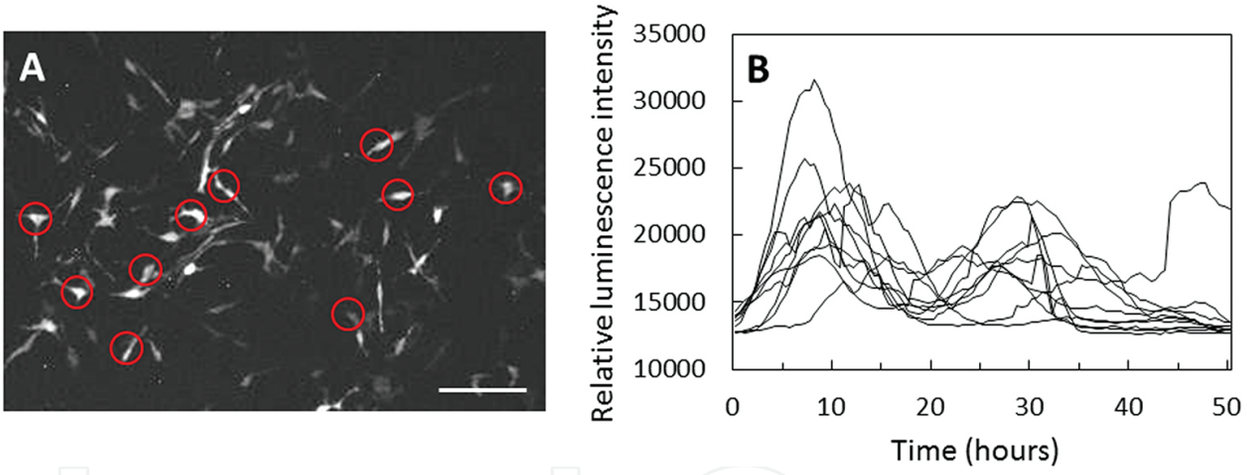

Figure 9. Bioluminescence image of *Per2* gene expression in NIH 3T3 cells using a *Luc*+ luciferase promoter vector (A). Time course of light intensity of the single cells (B). Images were captured using an LV200 microscope with an UPlanApo 20× objective lens and a DP30 CCD camera. Cells were stimulated with 1 mM dexamethasone. D-Luciferin, 500 μM. Exposure time, 5 min. Scale bar, 200 μm.

Figure 9 shows an example of imaging of *Per2* clock gene promoter activity in cultured cells. The promoter region of the *Per2* clock gene in mice was inserted into the luciferase promoter vector, pGL3 (Promega), and the vector was transfected into NIH3T3 cells. Cells were cultured in CO_2-independent DMEM (Invitrogen) containing 500 μM D-luciferin. Bioluminescence images were captured using an LV200 microscope with an UPlanApo 20× OB (NA = 0.70) and DP30BW CCD camera (Olympus) at 37°C. The binning of the CCD was 1 × 1 (1024 × 1024 pixels), the cooling temperature of the sensor chip was 5°C, and the exposure time was 5 min with 30-min interval for 28 h. As shown in **Figure 9A**, bioluminescence images of single cells expressing the *Per2* gene were captured clearly using a conventional CCD camera. **Figure 9B**

shows a time course of *Per2* promoter activity in 10 cells selected appropriately for 48 h using TiLIA [46]; this time course allowed us to analyze synchronicity among cells [49]. Using this imaging system, Ukai et al. [23] produced photoresponsive mammalian cells by introducing the photoreceptor melanopsin and monitored the effects of photoperturbation on the state of the cellular clock. They observed that a critical light pulse drove cellular clocks into singularity behavior and proved that loss of the circadian rhythm of a cellular clock may be caused by dis-synchronization of individual cells underlying singularity behavior by single-cell analysis.

3.3. Three-dimensional imaging of *Drosophila larva*

Because our bioluminescence microscope system utilizes a short-focal-length imaging lens, the magnification is lower and the focal depth is shallower than those of conventional microscopy systems using the same OB. Therefore, depth of field is also shallower. This is convenient for three-dimensional image reconstruction by light sectioning.

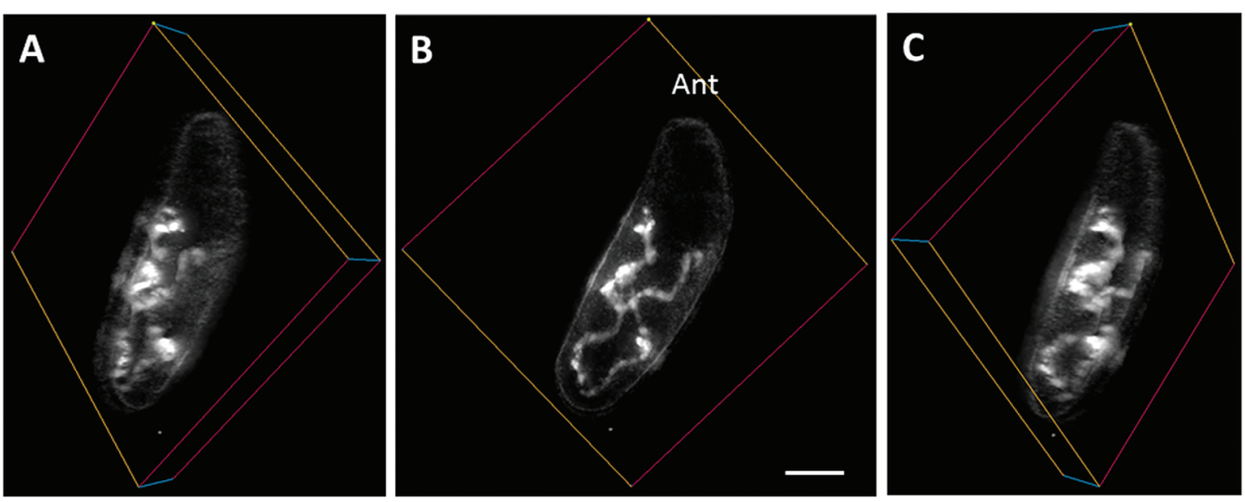

Figure 10. Three-dimensional bioluminescence image of armadillo promoter activity of insular larva for the transgenic *Drosophila melanogaster* reconstructs from 11 sectionalized images (100 μm depth). Expression of *armadillo* was observed in the midgut from a tissue depth of 100 μm. The larva was immersed in 3 mM D-luciferin for 5 min before image acquisition. A and C, slant view. B, front view. Scale bar, 100 μm. Ant, anterior part of the body.

Accordingly, we constructed transgenic *Drosophila melanogaster* carrying an armadillo (a member of the segment polarity gene) promoter and luciferase fusion gene [31]. **Figure 10** shows three-dimensional images of armadillo promoter activity from insular larva of transgenic flies reconstructed from 11 sectionalized images (front and slant views). The larva was immersed in 3 mM D-luciferin for 5 min before image acquisition. Bioluminescence images of the anesthetized larva with cold treatment were captured using an LV200 microscope with an UPlanFLN 60× OB (NA = 0.90) and iXon EM-CCD camera. The binning of the CCD was 1 × 1; EM gain was maximum; and exposure time was 30 s. Eleven sectionalized images were obtained with 10-μm steps from top to bottom (0–100 μm) of the larva. After deconvolution, three-dimensional images were reconstructed using CelSens Dimension image analysis software (Olympus). As shown in the **Figure 10**, the expression of the *armadillo* was observed

in the midgut from a tissue depth of 100 μm, although it needed clearing treatment of kidney tissue for imaging of 100–200 mm depth by confocal fluorescence microscopy [50].

4. Conclusion

In this study, we presented the concept of bioluminescence microscopy using a short-focal-length IM. This system facilitates the acquisition of bioluminescence images of single live cells using luciferase, similar to fluorescence microscopy using a fluorescent protein, although M is lower than that of conventional microscopy. Furthermore, this method is applicable for studies of cellular activity at the single cell level, including analyses of signal transduction, gene expression, and embryogenesis.

As bioluminescence microscopy requires no excitation light, it leads to substantive differences from fluorescence microscopy. Bioluminescence observation lacks the phototoxicity and background autofluorescence problems associated with fluorescence observation and permits the long-term, non-lethal observation of living cells such as embryonic stem cells, iPS cells, and embryos. **Table 1** summarized the substantive differences between the fluorescence and bioluminescence microscopy. Thus, bioluminescence microscopy is a powerful tool in cellular biology and complements fluorescence microscopy.

	Fluorescence	**Bioluminescence**
Excitation energy	Photon	Chemical reaction
Auto-fluorescence	Affected	None
Phototoxicity	Affected	None
Long-term observation	Acceptable	Excellent
Observation of photosensitive cell	Acceptable	Excellent
Brightness of image	Excellent	Acceptable
Spatiotemporal resolution	Excellent	Acceptable

Table 1. Substantive differences between fluorescence and bioluminescence microscopy.

Acknowledgements

We thank Drs. ES Vysotski (Russian Academy of Science) and Y Nakajima (National Institute of Advanced Industrial Science and Technology, Dr. Ohmiya's Lab) for providing plasmid vectors, apoobelin, and the Per2 reporter. We also thank our colleagues at Olympus Corporation for technical assistance and discussion during the development of bioluminescence microscope, LV200.

Author details

Hirobumi Suzuki[1*], May-Maw-Thet[1,2], Yoko Hatta-Ohashi[1], Ryutaro Akiyoshi[1] and Taro Hayashi[1]

*Address all correspondence to: hirobumi2_suzuki@ot.olympus.co.jp

1 Evaluation Technology Department 1, Olympus Corporation, Hachioji, Tokyo, Japan

2 Department of Experimental Animal Model for Human Disease, Graduate School of Medical and Dental Sciences, Tokyo Medical and Dental University, Tokyo, Japan

References

[1] Shimomura O, Johnson FH, Saiga Y. Extraction, purification and properties of aequorin, a bioluminescent protein from hydromedusan *Aequorea*. J. Cell. Comp. Physiol. 1962; 59:223–239.

[2] Ridgway EB, Gilkey JC, Jaffe LF. Free calcium increases explosively in activating medaka eggs. Proc. Nat. Acad. Sci. U. S. A. 1977; 74:623–627.

[3] Gilkey JC, Jaffe LF, Ridgway EB, Reynolds GT. A free calcium wave traverses the activating egg of the medaka, *Oryzias latipes*. J. Cell Biol. 1978; 76:448–466.

[4] Yamamoto T. Physiology of fertilization in fish eggs. Int. Rev. Cytol. 1961; 12:361–405.

[5] de Wet JR, Wood KV, DeLuca M, Helinski DR, Subramani S. Firefly luciferase gene: structure and expression in mammalian cells. Mol. Cell Biol. 1987; 7:725–735.

[6] Brasier AR, Tate JE, Habener JF. Optimized use of the firefly luciferase assay as a reporter gene in mammalian cell lines. BioTechniques. 1989; 7:1116–1122.

[7] Alam J, Cook JL. Reporter genes: application to the study of mammalian gene transcription. Anal. Biochem. 1990; 188:245–254.

[8] Frawley LS, Faught WJ, Nicholson J, Moomaw B. Real time measurement of gene expression in living endocrine cells. Endocrinology. 1994; 135:468–471.

[9] Thompson EM, Adenot P, Tsuji FI, Renard JP. Real time imaging of transcriptional activity in live mouse preimplantation embryos using a secreted luciferase. Proc. Natl. Acad. Sci. U. S. A. 1995; 92:1317–1321.

[10] White MRH, Masuko M, Amet L, Elliott G, Braddock M, Kingsman AJ, Kingsman SM. Real-time analysis of the transcriptional regulation of HIV and hCMV promoters in single mammalian cells. J. Cell Sci. 1995; 108:441–455.

[11] Castaño JP, Kineman RD, Frawley LS. Dynamic monitoring and quantification of gene expression in single, living cells: a molecular basis for secretory cell heterogeneity. Mol. Endocrinol. 1965; 10:599–605.

[12] Kennedy HJ, Viollet B, Rafiq I, Kahn A, Rutter GA. Upstream stimulatory factor-2 (USF2) activity is required for glucose stimulation of L-pyruvate kinase promoter activity in single living islet β-cells. J. Biol. Chem. 1997; 272:20636–20640.

[13] Takasuka N, White MRH, Wood CD, Robertson WR, Davis JRE. Dynamic changes in prolactin promoter activation in individual living lactotrophic cells. Endocrinology. 1998; 139:1361–1368.

[14] Maire E, Lelièvre E, Brau D, Lyons A, Woodward M, Fafeur V, Vandenbunder B. Development of an ultralow–light–level luminescence image analysis system for dynamic measurements of transcriptional activity in living and migrating cells. Anal. Biochem. 2000; 280:118–127.

[15] Welsh DK, Yoo SH, Liu AC, Takahashi JS, Kay SA. Bioluminescence imaging of individual fibroblasts reveals persistent, independently phased circadian rhythms of clock gene expression. Curr. Biol. 2004; 14:2289–2295.

[16] Masamizu Y, Ohtsuka T, Takashima Y, Nagahara H, Takenaka Y, Yoshikawa K, Okamura H, Kageyama R. Real-time imaging of the somite segmentation clock: revelation of unstable oscillators in the individual presomitic mesoderm cells. Proc. Natl. Acad. Sci. U. S. A. 2006; 103:1313–1318.

[17] Hoshino H, Nakajima Y, Ohmiya Y. Luciferase-YFP fusion tag with enhanced emission for single-cell luminescence imaging. Nat. Methods. 2007; 4:637–639.

[18] Kwon HJ, Enomoto T, Shimogawara M, Yasuda K, Nakajima Y, Ohmiya Y. Bioluminescence imaging of dual gene expression at the single-cell level. BioTechniques. 2010; 48:460–462.

[19] Suzuki T, Kondo C, Kanamori T, Inouye S. Video rate bioluminescence imaging of secretory proteins in living cells: localization, secretory frequency, and quantification. Anal. Biochem. 2011; 415:182–189.

[20] Suzuki H, Dosaka S, Ohashi-Hatta Y, Sugiyama T. Luminescence microscope for reporter assay of single live cells. In: Proceedings of the 14th International Symposium on Bioluminescence and Chemiluminescence Chemistry, Biology, and Applications; 15–19 Oct 2006; San Deago. Singapore: World Scientific; 2007. pp. 53–56.

[21] Ogoh K, Akiyoshi R, May-Maw-Thet, Sugiyama T, Dosaka S, Hatta-Ohashi Y, Suzuki H. Bioluminescence microscopy using a short focal-length imaging lens. J. Microsc. 2014; 253:191–197.

[22] Sato TK, Yamada RG, Ukai H, Baggs JE, Miraglia LJ, Kobayashi TJ, Welsh DK, Kay SA, Ueda HR, Hogenesch JB. Feedback repression is required for mammalian circadian clock function. Nat. Genet. 2006; 38:312–319.

[23] Ukai H, Kobayashi TJ, Nagano M, Masumoto K, Sujino M, Kondo T, Yagita K, Shigeyoshi Y, Ueda HR. Melanopsin-dependent photo-perturbation reveals desynchronization underlying the singularity of mammalian circadian clocks. Nat. Cell Biol. 2007; 9:1327–1334.

[24] Akashi M, Hayasaka N, Yamazaki S, Node K. Mitogen-activated protein kinase is a functional component of the autonomous circadian system in the suprachiasmatic nucleus. J. Neurosci. 2008; 28:4619–4623.

[25] Dibner C, Sage D, Unser M, Bauer C, d'Eysmond T, Naef F, Schibler U. Circadian gene expression is resilient to large fluctuations in overall transcription rates. EMBO J. 2008; 28:123–134.

[26] Fukuda H, Tokuda I, Hashimoto S, Hayasaka N. Quantitative analysis of phase wave of gene expression in the mammalian central circadian clock network. PLoS One. 2011; 6:e23568, 1–8.

[27] Yagita K, Horie K, Koinuma S, Nakamura W, Yamanaka I, Urasaki A, Shigeyoshi Y, Kawakami K, Shimada S, Takeda J, Uchiyama Y. Development of the circadian oscillator during differentiation of mouse embryonic stem cells in vitro. Proc. Natl. Acad. Sci. U. S. A. 2010; 107:3846–3851.

[28] Edwards MD, Brancaccio M, Chesham JE, Maywood ES, Hastings MH. Rhythmic expression of cryptochrome induces the circadian clock of arrhythmic suprachiasmatic nuclei through arginine vasopressin signaling. Proc. Natl. Acad. Sci. U. S. A. 2016; 113:2732–2737.

[29] Asai S, Takamura K, Suzuki H, Setou M. Single-cell imaging of *c-fos* expression in rat primary hippocampal cells using a luminescence microscope. Neurosci. Lett. 2008; 434:289–292.

[30] Chang E, Pohling C, Natarajan A, Witney TH, Kaur J, Xu L, et al. AshwaMAX and Withaferin A inhibits gliomas in cellular and murine orthotopic models. J. Neurooncol. 2016; 126:253–264.

[31] Akiyoshi R, Kaneuch T, Aigaki T, Suzuki H. Bioluminescence imaging to track real-time armadillo promoter activity in live *Drosophila* embryos. Anal. Bioanal. Chem. 2014; 406:5703–5713.

[32] Sramek C, Mackanos M, Spitler R, Leung LS, Nomoto H, Contag CH, Palanker D. 2011. Non-damaging retinal phototherapy: dynamic range of heat shock protein expression. Invest. Opthalmol. Vis. Sci. 2011; 52:1780–1787.

[33] Horibe T, Torisawa A, Akiyoshi R, Hatta-Ohashi Y, Suzuki H, Kawakami K. Transfection efficiency of normal and cancer cell lines and monitoring of

promoter activity by single-cell bioluminescence imaging. Luminescence. 2014; 29:96–100.

[34] Horibe T, Torisawa A, Kurihara R, Akiyoshi R, Hatta-Ohashi Y, Suzuki H, Kawakami K. Monitoring Bip promoter activation during cancer cell growth by bioluminescence imaging at the single-cell level. Integr. Cancer Sci. Therap. 2015; 2:291–299.

[35] Kikuchi O, Ohashi S, Horibe T, Kohno M, Nakai Y, Miyamoto S, Chiba T, Muto M, Kawakami K. Novel EGFR-targeted strategy with hybrid peptide against oesophageal squamous cell carcinoma. Sci. Rep. 2016; 6:22452, 1–12.

[36] Rogers KL, Martin JR, Renaud O, Karplus E, Nicola MA, Nguyen M, Picaud S, Shorte SL, Brûlet P. Electron-multiplying charge-coupled detector-based bioluminescence recording of single cell Ca^{2+}. J. Biomed. Optics. 2008; 13:031211, 1–10.

[37] Hall MP, Unch J, Binkowski BF, Valley MP, Butler BL, Wood MG, Otto P, Zimmerman K, Vidugiris G, Machleidt T, Robers MB, Benink HA, Eggers CT, Slater MR, Meisenheimer PL, Klaubert DH, Fan F, Encell LP, Wood KV. Engineered luciferase reporter from a deep sea shrimp utilizing a novel imidazopyrazinone substrate. ACS Chem. Biol. 2012; 7:1848–1857.

[38] Sugiyama T, Suzuki H, Takahashi T. Light-induced rapid Ca^{2+} response and MAPK phosphorylation in the cells heterologously expressing human OPN5. Sci. Rep. 2014; 4:5352, 1–10.

[39] Binkowski B, Fan F, Wood K. Engineered luciferases for molecular sensing in living cells. Curr. Opin. Biotechnol. 2009; 20:14–18.

[40] Cosby N. Enabling kinetic studies of GPCRs. Live-cell, non-lytic biosensor for GPCR profiling. Screening. 2009; 4:28–29.

[41] Compan V, Pierredon S, Vanderperre B, Krznar P, Marchiq I, Zamboni N, Pouyssegur J, Martinou JC. Monitoring mitochondrial pyruvate carrier activity in real time using a BRET-based biosensor: investigation of the Warburg effect. Mol Cell. 2015; 59:491–501.

[42] Pratx G, Chen K, Sun C, Martin L, Carpenter CM, Olcott PD, Xing L. Radioluminescence microscopy: measuring the heterogeneous uptake of radiotracers in single living cells. PLoS One. 2012; 7:e46285, 1–9.

[43] Pratx G, Chen K, Sun C, Axente M, Sasportas L, Carpenter C, Xing L. High-resolution radioluminescence microscopy of 18F-FDG uptake by reconstructing the β-ionization track. J. Nucl. Med. 2013; 54:1841–1846.

[44] Goda K, Hatta-Ohashi Y, Akiyoshi R, Sugiyama T, Sakai I, Takahashi T, Suzuki H. Combining fluorescence and bioluminescence microscopy. Microsc. Res. Tech. 2015; 78:715–722.

[45] Marcova SV, Vysotski ES, Blinks JR, Burakova LP, Wang BC, Lee J. Obelin from the bioluminescent marine hydroid *Obelia geniculate*: cloning, expression, and comparison

of some properties with those of other Ca^{2+}-regulated photoproteins. Biochemistry. 2002; 41:2227–2236.

[46] Konno J, Hatta-Ohashi Y, Akiyoshi R, Thancharoen A, Silalom S, Sakchoowong W, Yiu V, Ohba N, Suzuki H. TiLIA: a software package for image analysis of firefly flash patterns. Ecol. Evol. 2016; 6:3026–3031.

[47] May-May-Thet, Sugiyama T, Suzuki H. Bioluminescence imaging of intracellular calcium dynamics by the photoprotein obelin. In: Proceedings of the 15th International Symposium on Bioluminescence and Chemiluminescence Light Emission: Biology and Scientific Applications; 13–17 May 2008; China. Singapore: World Scientific; 2009. pp. 359–362.

[48] Olympus. Intracellular calcium imaging using photoprotein, obelin. 2009. Available from: http://bioimaging.jp/appli/007/pdf/app_lv200.pdf [Accessed: 2016-06-06]

[49] Olympus. Imaging of clock gene promoter assay of culture cells. 2009. Available from: http://bioimaging.jp/appli/004/pdf/app_lv200.pdf [Accessed: 2016-06-06]

[50] Clendenon SG, Young PA, Ferkowicz M, Phillips C, Dunn KW. Deep tissue fluorescent imaging in scattering specimens using confocal microscopy. 2011; Microsc. Microanal. 17:614–617.

IntechOpen